

The Nuclear Fragmentation Phase Transition and Rare Isotope Production

Wolfgang Bauer^a, Scott Pratt, Christopher Morling, and Patrick Underhill^b

National Superconducting Cyclotron Laboratory,
and Department of Physics and Astronomy,
Michigan State University,
East Lansing, MI 48824-1321, USA

Abstract. Of all phase transitions in nuclear matter, the fragmentation phase transition is perhaps the one for which there is the best experimental evidence as of now. In addition, theoretical models have been developed to a degree where detailed comparisons are possible. With the advent of rare isotope production facilities using projectile fragmentation techniques (NSCL, GSI, . . . , and hopefully RIA in the coming decade), the main interest in this field is beginning to shift towards the exploration of the isospin degree of freedom in the nuclear equation of state. Here we employ a statistical multifragmentation model and discuss the connection between the width of the isotope distribution and the isospin term in the nuclear equation of state.

1. Introduction

The most interesting goal of high-energy heavy ion physics over the last two decades has been the exploration of the nuclear phase diagram, i.e. the response of nuclei and nuclear matter as a function of the thermodynamic variables density, pressure, and temperature.

There are two distinct phase transitions that theory predicts to exist in this nuclear matter phase diagram. The first is the transition between a plasma of quarks and gluons and a gas of (color-singlet) hadrons. It dominated the early history of the universe about a microsecond after the Big Bang. The heavy ion program at CERN SPS, the AGS, and now at RHIC is attempting to recreate this transition in laboratory experiments. The other transition is that between a hadron gas and the Fermi liquid of ground state nuclei. This transition has been investigated at, among

others, our own facility, the National Superconducting Cyclotron Laboratory. It is of relevance, for example, in the astrophysical production of heavy elements [1].

It is by no means assured that we are actually able to investigate these phase transitions in laboratory experiments. In order to be able to use the terminology of thermodynamics, we need to establish that equilibrium has indeed been established. In addition, there is no possibility to prepare our nuclear system in a certain state at fixed values of the thermodynamic variables and keep it there for measurements. The hot nuclear matter that we create in heavy ion collisions instead will propagate along a path through the phase diagram. And since we are relegated to only measuring asymptotic momentum states of particles produced in these heavy ion collisions, it is not even clear that we can extract values for the thermodynamic variables.

However, during the last two decades the field of heavy ion physics has made astounding progress in answering many of these questions. For example, the question of measuring the volume has been studied intensively by using Hanbury-Brown-Twiss type of intensity interferometry [2].

Here we will describe recent advances in our understanding of the fragmentation phase transition and the future extension of these studies into the isospin degree of freedom.

2. Percolation Model

One model that has been employed to study the physics of the fragmentation phase transition is the percolation model [3], in particular the formulation of nuclear fragmentation as a 3d bond percolation problem. One particularly interesting feature of the percolation model is that it contains a continuous phase transition. In the limit of infinite lattices one can show that the critical exponents are not dependent on the particular lattice structure employed, and from the numerical value of the critical exponents it is observed that hyperscaling,

$$2 - \alpha = (\tau - 1)/\sigma = 2\beta + \gamma \quad (1)$$

seems to hold. The critical exponent β is defined from the relation $P \propto (p - p_c)^\beta$ for the order parameter as a function of the control parameter and has the numerical value of $\beta = 0.41$. The exponent γ governs the divergence of the cluster size distribution at the critical point, $\propto |p - p_c|^{-\gamma}$, and has the numerical value of $\gamma = 1.8$.

In our percolation-based model, one recognizes that the strong interaction is short-ranged, and that are nucleons connected with their nearest neighbors. Deposition of excitation energy results in broken bonds as the nuclei expand. The physics of the energy deposition then enters into the determination of the bond existence or, equivalently, breaking probability. For proton-induced multifragmentation, the Glauber approximation has been employed successfully. Here, the energy deposition into the target and the breaking probability is determined as a function of

the impact parameter by the number of nucleons encountered by the projectile on its path through the target nucleus. This model has been able to reproduce the experimentally observed U-shaped mass distributions, overall fragmentation cross sections, and low-to-medium-mass power laws of the cross sections for a wide variety of target nuclei in the limiting fragmentation beam energy domain.

For heavy ion collisions, the Glauber approximation as a means to calculate energy deposition is clearly no longer sufficient. Instead we have constructed a hybrid model [4] with a first stage intranuclear cascade step that calculates excitation energy and size of the residue and a second stage percolation step. The excitation energy deposition is related to the bond breaking probability via [5]

$$p_b(T) = 1 - \frac{2}{\sqrt{\pi}} \Gamma\left(\frac{3}{2}, 0, \frac{B}{T}\right), \quad (2)$$

where Γ is the generalized incomplete gamma function, B is the binding energy per nucleon in the residue (taken as 6 MeV here), and T is the temperature. This prescription is a generalization of the Coniglio-Klein formula for the existence of a bond between neighboring sites [6, 7]

$$p_{CK} = 1 - \exp(-\mathcal{E}/2T) \quad (3)$$

where \mathcal{E} is the nearest-neighbor interaction energy. Thus there is a close connection between the bond percolation theory and the lattice gas model.

Recently, the EoS collaboration [8–10] has attempted to measure the critical exponents β and γ that determine the universality class of the nuclear fragmentation phase transition directly in the reaction of 1 A·GeV Au + C reactions, by using a TPC to ensure full reconstruction of all 79 charges of the gold nucleus. They measured the second moment of the charge distribution,

$$M_2 = \sum_{k=1}^{\infty'} k^2 n(k) \propto |p_b - p_c|^{-\gamma} \quad (4)$$

(The upper limit in this sum is meant to indicate that the largest fragment – the “infinite cluster” – is not included) on an event-by-event basis as a function of the total charged particle multiplicity. They extracted values of $\gamma = 1.4$, $\beta = 0.29$.

In Fig. 1, the data of the EoS collaboration are shown by the filled plot symbols (statistical error bars are present, but smaller than the plot symbols). For each multiplicity, two values of M_2 are shown, the upper one where the summation in Eq. 4 includes all fragments, and the lower one where the largest fragment was excluded. Also shown is the power-law fit to the data (thin smooth line) that led to the extraction of the values for γ and β just quoted. The power-law fits were adjusted to reproduce the data points within the gray shaded rectangles in Fig. 1. Also shown in this figure is the result of our calculations with the percolation hybrid model (histogram). Almost perfect agreement is obtained for all multiplicities. Since this model has no adjustable fit parameters, this agreement has to be called

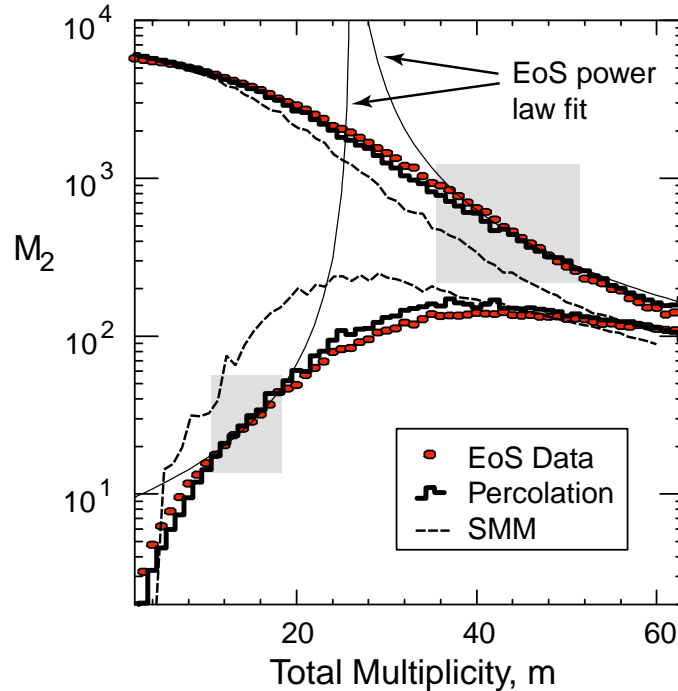


Fig. 1. Comparison of the EoS data [8–10] (filled circles) with the percolation model (histogram) and the SMM model of Botvina et al. (dashed line) [4]. The thin smooth curves represent the power-law fit of the EoS collaboration, and the grey rectangles mark the data points that were used for the fit. The upper curves and data points are for the second moments as calculated by using all fragments, and the lower curves by using all but the heaviest fragment.

impressive. For comparison, we also show the result of the calculations using the SMM [11] (dashed line), where very clear deviations from the data can be seen.

We conclude from this comparison that the data of the carbon induced multifragmentation of gold indeed contain significant circumstantial evidence for a second order phase transition in nuclear matter, and that the universality class of this phase transition is that of percolation, with $\gamma = 1.8$, $\beta = 0.41$.

3. Fragmentation of Molecules

Possibly the most interesting feature of nuclear fragmentation is that it gives us a glimpse on the modifications that extreme finite-size effects cause for the character of a phase transition. This is one area where this particular subfield can be expected

to have a major impact on general many-body science.

Another field in which similar investigations can be made is that of molecular fragmentation. Indeed, experiments recently performed at Argonne National Laboratory for the fragmentation of buckyballs (C_{60} -fullerenes) have also shown fragmentation patterns very similar to those observed in high-energy proton-induced nuclear multifragmentation experiments. However, the space available here does not allow us to elaborate, and we refer to the literature [12].

4. Isospin

The study of rare isotopes is attracting increasing attention due to the recent development of radioactive beam facilities where isotopes are produced through nuclear collisions. Projectile and target nuclei might vary in size from a few dozen nucleons all the way to Uranium. The mechanism for rare isotope production might entail the transfer of a few nucleons between the projectile and target, induced fission of the projectile, or at highest energy transfer, multifragmentation. This last mechanism, which assumes temperatures of a few MeV, is the focus of this study [13].

Isospin effects have been studied in lattice-gas models [14, 15] and in percolation [16, 17]. Recently, Xu et al. have measured yields of light fragments from the fragmentation of both ^{112}Sn and ^{124}Sn , and by taking ratios of isotope yields have determined the relative chemical potentials of the two systems [18]. In our percolation studies [16], we found that we were not able to reproduce the detailed values of the isospin shifts observed in experiment. In a more purely theoretical study for multicomponent percolation systems, however, Harreis and W.B. found that these can be reduced to one-component percolation problems, albeit with a remarkable shift in the critical percolation probability value in some limiting cases [17].

In the present manuscript we will from here on focus on the canonical ensemble and utilize the statistical model, combined with a simulation of sequential decay. Since our goal is to study the yields of rarely produced isotopes which may be produced in future radioactive beam facilities as rarely as in one per 10^{17} events, we employ the methods recently promoted by Chase and Mekjian [19–21] which forego the need of using Monte Carlo methods. Majumder and Das Gupta have in fact studied Boron, Carbon and Nitrogen isotope production with a similar model to what is presented here [22]. The disadvantage of this method is that explicit interaction of fragments (beyond mean field or excluded volume effects) is outside the scope of the formalism.

The recursion relation for the canonical distribution function is

$$\begin{aligned}\Omega_{Z,N}(T) &= \sum_c e^{-\beta E_c} \\ &= \sum_i \frac{a_i}{A} \omega_i(T) \Omega_{Z-z_i, N-n_i}(T),\end{aligned}\tag{5}$$

where the label c in the summation in the first line indicates one particular config-

uration, and ω_i is the partition function of a specific nuclear species i ,

$$\omega_i(T) = \frac{V_{\text{red}}(m_i T)^{3/2}}{(2\pi)^{3/2}} \sum_{\text{internal levels } j} e^{-\beta E_j}, \quad (6)$$

where m_i is the mass and z_i , n_i and a_i are the charge neutron number and baryon number of the species i . The reduced volume, $V_{\text{red}} = V_{\text{total}} - 2A/\rho_b$, roughly accounts for the overlap of the nuclei. Given the default breakup density of one sixth ρ_0 , the resulting reduced volume is four times the volume of a system at normal nuclear density.

Calculating the partition functions of specific species ω_i is straightforward given the levels and degeneracies of the nuclei. This was done for all fragments with $a < 6$. However, many of the nuclei which are generated in this approach have not yet been observed, and for almost all of them the level structure is not known. Given our lack of understanding of the ground state energies, let alone the excited state energies, we employ a liquid-drop treatment. We have chosen the finite-range liquid-drop model (FRLDM) [23] as a means for generating ground state energies and have ignored the microscopic terms in the model which account for shell structure. The spectrum of excited states was generated by assuming a uniformly spaced assortment of single-particle states with spacing $\Delta E = \alpha/\sqrt{A}$, where α is the level density parameter, chosen to be 10 MeV. The degeneracy of a state with excitation energy $n\Delta E$ was found by counting all ways to arrange particles and holes such that they summed to the desired excitation energy. For heavy nuclei, the separation ΔE becomes small, and when the separation fell below one MeV, the spectrum is interpolated onto a mesh of 1.0 MeV resolution. Finally, all mass-formula energies were modified to account for screening of the Coulomb potential,

$$E_{\text{coul.}} \rightarrow E_{\text{coul.}}(1 - \rho/\rho_0), \quad (7)$$

where ρ/ρ_0 is the ratio of the density to nuclear matter density.

The vast majority of the nuclear levels considered in these calculations are particle-unstable, including the ground states of those species outside the proton and neutron drip lines. After the initial yields were calculated, the subsequent decay was modeled by apportioning the weight of an unstable level into all the levels into which the nucleus might decay. Eight decay modes were considered: proton, neutron, deuteron, dineutron, diproton, t, ^3He and α . The decay weights were chosen according to Weisskopf arguments. Decays were calculated for all levels in all nuclei, beginning with the heaviest nuclei. For the decay of each level, the decay rate was calculated into every possible level energetically accessible through the eight decay modes listed previously. The weight associated with the decaying nucleus was then apportioned into all the states in proportion to the rates for the decay into such states. The weights were also simultaneously added into the ground states of the eight nuclei representing the eight decay modes. Thus, the decaying process exactly preserved the initial N and Z of the original system.

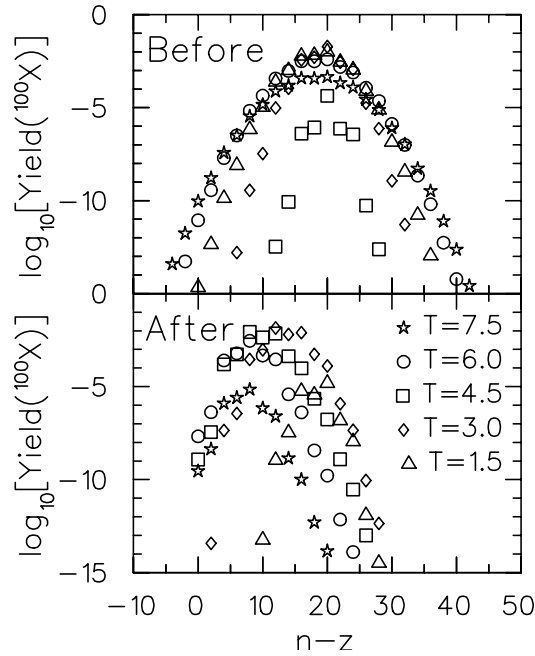


Fig. 2. Yields of mass 100 fragments are shown for the fragmentation of an $A = 200$, $Z = 80$ system at a variety of temperatures. Yields are shown both for the case where sequential decay is included (lower panel) and neglected (upper panel) [13].

While the width of the isotope distribution is sensitive to the isospin term in the nuclear equation of state, in practice the influence of sequential decays obscures this effect. To illustrate this statement, we show in Fig. 2 a comparison of the isotope production yields before (upper panel) and after (lower panel) sequential decays for several temperatures.

By considering yields of fragments of a fixed a as a function of $n - z$, two lessons were learned by considering a simple liquid drop model. First, the width of the initial distribution was determined largely by the ratio of the temperature to the symmetry term in the liquid-drop model. Secondly, isospin amplification, or isospin fractionation, could also be simply understood in terms of the same two quantities.

Sequential decay dramatically altered the yields, pushing the yields towards the valley of stability. The effects were strongest for larger fragments and for higher temperatures. As the initial distributions for fragments of fixed a as a function of $n - z$ were broadest at high temperature, inclusion of sequential decay shows that 5 MeV is the best temperature for creating rare neutron-rich fragments in the $a = 40$

region. For heavy fragments with $a = 100$, the optimum temperature was near three MeV which is more in the domain of fission than the domain of multifragmentation.

In order to understand the sensitivity of the calculations to various aspects of the modeling, the breakup density, level density, system size and system neutron fraction were systematically varied. Results were weakly dependent on the breakup density and moderately sensitive to the level density. Larger systems lead to somewhat broader yields due to finite-size constraints. Yields were especially sensitive to small changes in the isospin composition of the overall system. Thus, choosing projectiles and targets with large neutron fractions, e.g. N/A for Uranium is 0.614 and N/A for ^{124}Sn is 0.597, strongly increases the chances of creating isotopes near the neutron drip line. Finally, the sensitivity of the yields with respect to details of the evaporation was considered by adjusting the Coulomb barrier that leads to preferential emission of neutrons as opposed to protons. The yields of neutron-rich fragments were surprisingly insensitive to the barrier and changed almost imperceptibly when the Coulomb barrier was removed altogether. Proton-rich fragments were however quite sensitive to the details, as the tunneling allowed proton-rich fragments to return to the valley of stability.

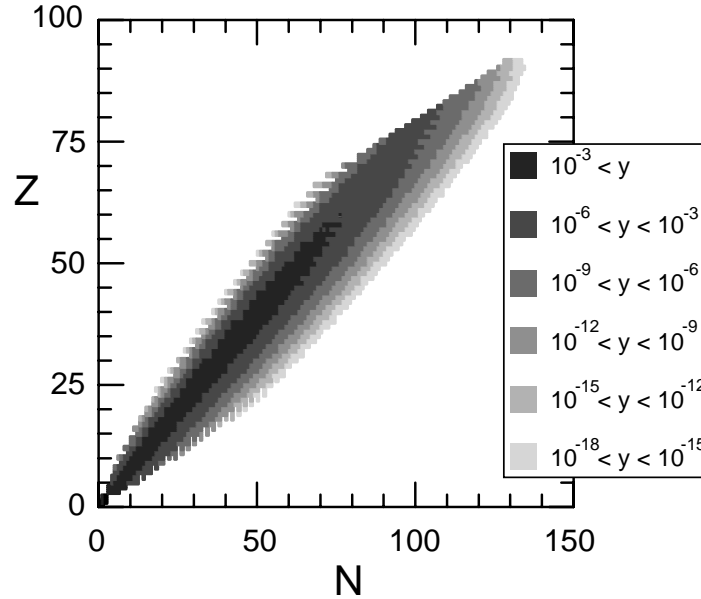


Fig. 3. Predictions of fragmentation isotope yield probabilities, y , (yields per fragmentation event) for the fragmentation of ^{238}U at a temperature of 4.5 MeV in our statistical multifragmentation model.

The ability of statistical models to explain isotope production is certainly of scientific interest in its own right. Additionally, one might also consider whether

multifragmentation could offer a competitive means for creating rare isotopes. In Fig. 3, we show as an example model calculations for isotope production probabilities, y , in the fragmentation of ^{238}U at a temperature of 4.5 MeV, a condition that can be achieved in projectile fragmentation.

What is shown in Fig. 3 should only be considered a first exploratory study. More detailed simulations of reaction dynamics effects are needed. In addition, separating and focusing particles could be problematic. If one fragmented heavy nuclei, which have the broadest yields, the Coulomb forces between the fragment of interest and various parts of the residual system would spread the emission over a large kinematic region making separation or focusing of the produced particles difficult. This would be especially true for fragments produced at mid-rapidity. Thus, it is difficult to discern whether there is a pragmatic side to the isospin degree of freedom in multifragmentation. To date, experiments that measure isotope yields have either been designed to focus on projectile rapidities and thus ignore multifragmentative events, or have measured production of light elements, $a < 20$. If statistical descriptions are shown to accurately describe isotope production for a broader range of nuclides, it might warrant serious consideration of designing an apparatus to capture and identify very rare isotopes in a very different environment than projectile fragmentation.

Acknowledgements

Funding for this research was received from the National Science Foundation, grants PHY-9605207, INT-9981342, and PHY-0070818. Patrick Underhill was supported by the Research Experience for Undergraduates program at Michigan State University which is sponsored by the National Science Foundation, grants PHY-9424140 and PHY-9912212. Christopher Morling was supported by the Undergraduate Professorial Assistants Program at Michigan State University. In addition, Wolfgang Bauer received partial support from a U.S. Distinguished Senior Scientist Award from the German Alexander-von-Humboldt Foundation.

Notes

- a.* Email: bauer@pa.msu.edu
Homepage: <http://www.nsc1.msu.edu/~bauer/>
- b.* Current address: Department of Physics, Washington University, Campus Box 1105, One Brookings Drive, St. Louis, MO 63130

References

1. B.-A. Li, C.M. Ko, and W. Bauer, *Int. J. Mod. Phys. E* **7**(2), 147 (1998).
2. W. Bauer, C.K. Gelbke, and S. Pratt, *Annu. Rev. Nucl. Part. Sci.* **42**, 77 (1992); W. Bauer, *Prog. in Part. and Nucl. Phys.* **30**, 45 (1993).

3. W. Bauer et al., Phys. Lett. **150** B, 53 (1985); W. Bauer et al., Nucl. Phys. **A452**, 699 (1986); X. Campi, J. Phys. A **19**, L917 (1986); T. Biro et al., Nucl. Phys. **A459**, 692 (1986); J. Nemeth et al., Z. Phys. A **325**, 347 (1986).
4. W. Bauer and A. Botvina, Phys. Rev. C **52**, R1760 (1995); W. Bauer and A. Botvina, Phys. Rev. C **55**, 546 (1997).
5. T. Li et al., Phys. Rev. Lett. **70**, 1924 (1993); T. Li et al., Phys. Rev. C **49**, 1630 (1994).
6. A. Coniglio and Klein, J. Phys. A **13**, 2775 (1980)
7. X. Campi, X. and H. Krivine, Nucl. Phys. A **620**, 46 (1997).
8. J.B. Elliott et al., Phys. Rev. C **49**, 3185 (1994).
9. M.L. Gilkes et al., Phys. Rev. Lett. **73**, 1590 (1994).
10. H.G. Ritter et al., Nucl. Phys. A **583**, 491c (1995).
11. J.P. Bondorf, A.S. Botvina, A.S. Iljinov, I.N. Mishustin and K. Sneppen, Phys. Rep. **257**, 133 (1995).
12. T. LeBrun et al., Phys. Rev. Lett. **72**, 3965 (1994); R. Ali et al., Nuclear Instruments and Methods in Physics Research B **96**, 545 (1995); T. LeBrun et al., Nuclear Instruments and Methods in Physics Research B **98**, 479 (1995); S. Cheng et al., Phys. Rev. A **54**, 3182 (1996).
13. S. Pratt, W. Bauer, C. Morling, and P. Underhill, Phys. Rev. C, in print (2000).
14. J. Pan, S. Das Gupta and M. Grant, Phys. Rev. C **57**, 1839 (1998); S.K. Samaddar and S. Das Gupta, Phys. Rev. C **61**, 034610, 2000.
15. Ph. Chomaz and F. Gulminelli, Phys. Lett. **B447**, 221 (1999).
16. G. Kortemeyer, W. Bauer, and G.J. Kunde, Phys. Rev. C **55**, 2730 (1997).
17. H.M. Harreis and W. Bauer, Phys. Rev. B **62**, 8719 (2000).
18. H.S. Xu, et al., Phys. Rev. Lett. **85**, 716 (1999).
19. K.C. Chase and A.Z. Mekjian, Phys. Rev. C **52**, R2339(1995).
20. S. Das Gupta and A.Z. Mekjian, Phys. Rev. C **57**, 1361(1998).
21. S. Pratt and S. Das Gupta, Phys. Rev. C **62**, 044603 (2000).
22. A. Majumder and S. Das Gupta, Phys. Rev. C **61**, 034603 (2000).
23. P. Möller, J.R. Nix, W.D. Myers and W.J. Swiatecki, Atomic Data and Nuclear Data Tables **59**, 185 (1995).